Check for updates

View Article Online
View Journal

Analyst

Accepted Manuscript

This article can be cited before page numbers have been issued, to do this please use: A. El-Hawiet, Y. Chen, K. Shams-Ud-Doha, E. Kitova, P. I. Kitov, L. Bode, N. Hage, F. Falcone and J. Klassen, *Analyst*, 2017, DOI: 10.1039/C7AN01397C.

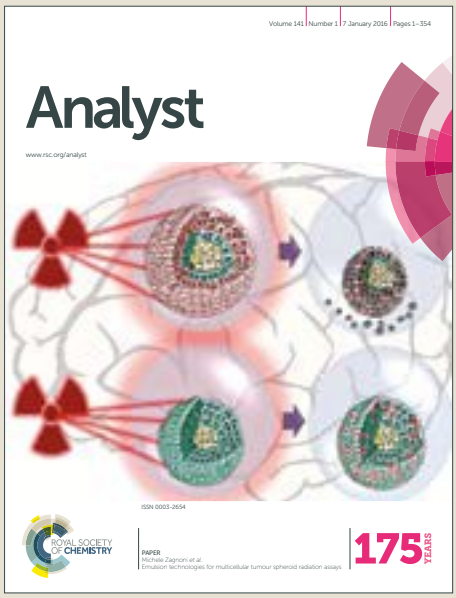

This is an Accepted Manuscript, which has been through the Royal Society of Chemistry peer review process and has been accepted for publication.

Accepted Manuscripts are published online shortly after acceptance, before technical editing, formatting and proof reading. Using this free service, authors can make their results available to the community, in citable form, before we publish the edited article. We will replace this Accepted Manuscript with the edited and formatted Advance Article as soon as it is available.

You can find more information about Accepted Manuscripts in the author guidelines.

Please note that technical editing may introduce minor changes to the text and/or graphics, which may alter content. The journal's standard Terms & Conditions and the ethical guidelines, outlined in our author and reviewer resource centre, still apply. In no event shall the Royal Society of Chemistry be held responsible for any errors or omissions in this Accepted Manuscript or any consequences arising from the use of any information it contains.

ROYAL SOCIETY OF CHEMISTRY

rsc.li/analyst

View Article Online
DOI: 10.1039/C7AN01397C

Published on 27 November 2017. Downloaded by University of Nottingham on 27/11/2017 21:14:28.

Screening Natural Libraries of Human Milk Oligosaccharides Against Lectins Using CaR-ESI-MS

Amr El-Hawiet,[1,2] Yajie Chen,[1] Km Shams-Ud-Doha,[1,§] Elena N. Kitova,[1] Pavel I. Kitov,[1] Lars Bode,[3] Naim Hage,[4] Franco H. Falcone[4] and John S. Klassen[1*]

[1]*Alberta Glycomics Centre and Department of Chemistry, University of Alberta, Edmonton, Alberta, Canada T6G 2G2*

[2]*Department of Pharmacognosy, Faculty of Pharmacy, Alexandria University, Alexandria, Egypt*

[3] *Division of Neonatology and Division of Gastroenterology and Nutrition, Department of Pediatrics, and Larsson-Rosenquist Foundation Mother-Milk-Infant Center of Research Excellence, University of California San Diego, CA*

[4]*School of Pharmacy, Division of Molecular Therapeutics and Formulation, University of Nottingham, Nottingham, United Kingdom, NG7 2RD*

* Corresponding Author:

Department of Chemistry

University of Alberta

Edmonton, AB CANADA T6G 2G2

Email: john.klassen@ualberta.ca

Telephone: (780) 492-3501

Fax: (780) 492 8231

Analyst Accepted Manuscript

View Article Online
DOI: 10.1039/C7AN01397C

Published on 27 November 2017. Downloaded by University of Nottingham on 27/11/2017 21:14:28.

§ *Current address: Sanford Burnham Prebys Medical Discovery Institute, 10901 North Torrey Pines Road, La Jolla, California 92037 USA*

Abstract

Human milk oligosaccharides (HMOs) afford many health benefits to breast-fed infants, such as protection against infection and regulation of the immune system, through the formation of non-covalent interactions with protein receptors. However, the molecular details of these interactions are poorly understood. Here, we describe the application of catch-and-release electrospray ionization mass spectrometry (CaR-ESI-MS) for screening natural libraries of HMOs against lectins. The HMOs in the libraries were first identified based on molecular weights (MWs), ion mobility separation arrival times (IMS-ATs) and collision-induced dissociation (CID) fingerprints of their deprotonated anions. The libraries were then screened against lectins and the ligands identified from the MWs, IMS-ATs and CID fingerprints of HMOs released from the lectin in the gas phase. To demonstrate the assay, four fractions, extracted from pooled human milk and containing ≥35 different HMOs, were screened against a C-terminal fragment of human galectin-3 (hGal-3C), for which the HMOs specificities have been previously investigated, and a fragment of the blood group antigen-binding adhesin (BabA) from *Helicobacter pylori*, for which the HMO specificities have not been previously established. The structures of twenty-one ligands, corresponding to both neutral and acidic HMOs, of hGal-3C were identified; all twenty-one were previously shown to be ligands for this lectin. The presence of HMO ligands at six other MWs was also ascertained. Application of the assay to BabA revealed nineteen specific HMO structures that are recognized by the protein and HMO ligands at two other MWs. Notably, it was found that BabA exhibits broad specificity for HMOs, and recognizes both neutral HMOs, including non-fucosylated ones, and acidic HMOs. The results of competitive binding

Analyst Accepted Manuscript

View Article Online
DOI: 10.1039/C7AN01397C

Published on 27 November 2017. Downloaded by University of Nottingham on 27/11/2017 21:14:28.

experiments indicate that HMOs can interact with BabA at previously unknown binding sites. The affinities of eight purified HMOs for BabA were measured by ESI-MS and found to be in the 10^3 M^{-1} to 10^4 M^{-1} range.

Introduction

Human milk, in addition to being an essential source of nutrition, provides infants with many important health benefits.[1,2] Human milk contains a variety of active components, including proteins, glycoproteins and fat globules.[3] Every liter of human milk also contains approximately 5 g to 25 g of unconjugated oligosaccharides, known as human milk oligosaccharides (HMOs).[4] Studies have shown that HMOs afford health benefits to breast-fed infants through several mechanisms.[5-7] They are known to have immune-stimulating effects and can influence the composition of microbiota in the gut and promote the growth of beneficial microorganisms.[8-10] HMOs can also protect newborns against infectious diseases by interfering with the binding of pathogenic bacteria and their toxins and viruses to intestinal epithelial cells.[11]

Central to the varied biological roles played by HMOs are the specific non-covalent interactions they form with endogenous and exogenous protein receptors. While their importance is well appreciated, the molecular details of these interactions are poorly understood. The large number of HMO structures found in human milk, including the presence of many structural isomers, and their wide ranging concentrations (~0.01 g L^{-1} to ~2 g L^{-1}) represent significant challenges to the comprehensive analysis of HMO interactions with proteins.[4,12] Of the more than two hundred known HMOs, fewer than fifty are commercially available.[13-17] Given the limited availability of purified HMOs, the use of mixtures of HMO, extracted directly from milk, is an attractive alternative for protein-HMO interaction studies. However, there are few screening technologies that are readily applied to natural libraries. One approach, pioneered by Cummings and co-workers, involves the use of shotgun glycan microarrays, which employ fractions of

Analyst Accepted Manuscript

View Article Online
DOI: 10.1039/C7AN01397C

Published on 27 November 2017. Downloaded by University of Nottingham on 27/11/2017 21:14:28.

HMOs, purified from human milk, that are chemically modified and immobilized on a solid surface.[18-20] The use of HMO glycan microarrays allows for the rapid profiling of HMO binding properties of lectins and the discovery of new protein-HMO interactions that might be relevant to human health. However, the derivatization of HMOs at the reducing end glucose is a drawback to this approach since the terminal lactose moiety is often implicated in the binding of HMOs to lectins.[21]

Electrospray ionization mass spectrometry (ESI-MS) is an attractive alternative to glycan microarrays for screening carbohydrate libraries against lectins *in vitro* and is particularly well suited for the study of HMO interactions since there is no requirement for labeling or immobilization of the oligosaccharides, which may influence their binding properties.[21] Direct detection and quantification of free and ligand-bound proteins ions by ESI-MS enables the binding stoichiometry and affinity of protein-carbohydrate interactions to be established.[22-26] Moreover, because it is possible to monitor multiple binding equilibria simultaneously, ESI-MS is also amenable to screening carbohydrate libraries.[27] In cases where the protein-carbohydrate complexes can't be detected or reliably quantified, library screening can be performed using a catch-and-release (CaR)-ESI-MS format, whereby ligands are identified following their release, as ions, from protein-ligand complexes upon collisional activation in the gas phase.[27] The assay is rapid, sensitive and label- and immobilization-free and, although not quantitative, can be used to identify the highest affinity ligands and to guide follow-up quantitative binding measurements.[27]

The CaR-ESI-MS assay has been previously used to screen a variety of defined oligosaccharide libraries, including free HMOs, and shown to successfully identify the highest affinity ligands in libraries containing in excess of two hundred different components.[28-34] Here,

Analyst Accepted Manuscript

View Article Online
DOI: 10.1039/C7AN01397C

Published on 27 November 2017. Downloaded by University of Nottingham on 27/11/2017 21:14:28.

we describe the application of the assay for screening mixtures of HMOs, extracted from pooled human milk, against lectins to identify specific ligands. To our knowledge, this represents the first demonstration of CaR-ESI-MS for screening natural libraries for protein interactions. The main advantage of using natural HMO libraries, compared to the libraries of purified HMOs, is the larger number and diversity of structures that are present, in particular the inclusion of larger oligosaccharides, which are not commercially available. A disadvantage is that it may not be possible to unambiguously assign the structures of all the extracted HMOs. However, even in cases where the exact structure is not known, the monosaccharide composition of the HMO ligand(s) can be readily established.

In the present study, the feasibility of using the CaR-ESI-MS assay to screen natural libraries of HMOs was demonstrated using a C-terminal fragment of human galectin-3 (hGal-3C), which contains the carbohydrate recognition domain, as a model HMO-binding lectin. The affinities of thirty-two free (unmodified) HMOs for hGal-3C were recently measured and these binding data served to validate the majority of the interactions identified by CaR-ESI-MS for the HMO libraries.[21] The assay was then used to screen the HMO libraries against a truncated form of the blood group antigen-binding adhesin (BabA) from *Helicobacter pylori* to evaluate its HMO specificities. This adhesin, one of approximately thirty outer membrane proteins, plays an important role in the association of *H. pylori* to the gastric mucosa.[35,36] BabA is known to recognize the fucosylated Lewis b histo-blood group antigen, Le^b and H1 terminal fucose residues on blood group O (H antigen), A and B antigens, salivary nonmucin glycoprotein gp-340, salivary mucin MUC5B and proline-rich glycoprotein.[35,36] Fucosylated glycans have been shown to inhibit *H. pylori* adhesion to human gastric tissue,[37] however, the HMO specificities of the adhesins have not been previously determined. Quantitative ESI-MS binding measurements,

Analyst Accepted Manuscript

View Article Online
DOI: 10.1039/C7AN01397C

Published on 27 November 2017. Downloaded by University of Nottingham on 27/11/2017 21:14:28.

performed on a subset of HMOs identified as ligands for BabA by the CaR-ESI-MS assay, served to validate the screening results. Competitive binding measurements were also carried out to establish whether BabA possesses previously unknown HMO binding sites.

Experimental Section

Proteins

The recombinant fragment of the C-terminus (residues 107–250) of human galectin-3 (hGal-3C, MW 16,330 Da) was a gift from Prof. C. Cairo (University of Alberta) and the recombinant truncated form (residues 21–547) of the blood group antigen-binding adhesin (BabA) from *Helicobacter pylori* strain *J99* ($BabA_{547}$, MW 58,211 Da) was produced and purified as described elsewhere.[38] Lysozyme (MW 14,310 Da), which served as the reference protein (P_{ref}), was purchased from Sigma-Aldrich Canada (Oakville, Canada). Each protein was dialyzed against 200 mM aqueous ammonium acetate (pH 6.8), concentrated using 10 kDa MW cut-off Amicon Ultra-4 centrifugal filters (Millipore Corp, Bedford, MA), and stored at -20 °C until used.

Human milk oligosaccharides

The structures of the pure HMOs are listed Table S1, Supporting Information. **HMO1** (MW 488.17 Da), **HMO2** (MW 488.17 Da), **HMO12** (MW 853.31 Da), **HMO13** (MW 853.31 Da), **HMO17** (MW 998.34 Da), **HMO20** (MW 999.36 Da), **HMO21** (MW 1072.38 Da), **HMO23** (MW 1144.40 Da), **HMO24** (MW 1144.40 Da), **HMO27** (MW 1364.50 Da) and **HMO28** (MW 1438.51 Da), **HMO29** (MW 545.48 Da), **HMO30** (MW 691.25 Da) and **HMO31** (MW 1056.39 Da) were purchased from Elicityl SA (Crolles, France); **HMO3** (MW 633.21 Da), **HMO4** (MW 633.21 Da), **HMO5** (MW 634.23 Da)**, HMO6** (MW 707.25 Da), **HMO7** (MW 707.25 Da), **HMO8** (MW 779.27 Da), **HMO9** (MW 853.31 Da), **HMO10** (MW 853.31 Da), **HMO11** (MW

Analyst Accepted Manuscript

View Article Online
DOI: 10.1039/C7AN01397C

Published on 27 November 2017. Downloaded by University of Nottingham on 27/11/2017 21:14:28.

853.31 Da), **HMO14** (MW 998.34 Da), **HMO15** (MW 998.34 Da), **HMO16** (MW 998.34 Da)**, HMO18** (MW 999.36 Da) and **HMO26** (MW 1364.50 Da) were purchased from IsoSep (Tullinge, Sweden); **HMO19** (MW 999.36 Da) and **HMO22** (MW 1072.38 Da) from Dextra (Reading, UK); **HMO25** (MW 1289.44 Da) was purchased from CarboSynth (Compton, UK). Stock solutions of each HMO were prepared by dissolving a known mass of the oligosaccharide in ultrafiltered water (Milli-Q, Millipore, Billerica, MA) to give a final concentration of 1 mM. All of the stock solutions were stored at -20 °C until used.

HMO fractions

Fourteen HMO fractions (designated as *Fraction 1 – Fraction 14*) were produced from pooled HMOs (pHMOs) originally isolated from human milk pooled from over 50 different donors with term infants. First, after centrifugation of the pooled human milk, the lipid layer was removed and proteins were precipitated from the aqueous phase by addition of ice-cold ethanol and subsequent centrifugation. Ethanol was removed from the HMO-containing supernatant by roto-evaporation. Lactose and salts were removed by gel filtration chromatography over a BioRad P2 column (100 cm316 mm, Bio-Rad, Hercules, California, USA) using a semi-automated fast protein liquid chromatography (FPLC) system. Second, pHMOs were separated by charge using anion exchange chromatography on an anion exchange column QAE Sephadex A-25 (Sigma-Aldrich, St. Louis, USA). Lyophilised pooled HMO were dissolved in 2 mM Tris and applied to equilibrated columns. Neutral HMOs were eluted with 2 mM Tris. Acidic HMOs were eluated with 2 mM Tris containing 200 mM NaCl. Afterwards, Tris and NaCl were removed from the neutral and acidic HMO fractions by gel filtration chromatography over a Bio-Gel P-2 gel filtration chromatography column (100 cm x 16 mm). Third, neutral and acidic HMO fractions

Analyst Accepted Manuscript

View Article Online
DOI: 10.1039/C7AN01397C

Published on 27 November 2017. Downloaded by University of Nottingham on 27/11/2017 21:14:28.

were further separated by size using Bio-Gel P-2 gel filtration chromatography (160 cm x 16 mm) with 10 mL subfraction resolution. All fractions were lyophilized for future use.

To prepare stock solutions, *Fraction 1*-*Fraction 14* (*Fraction 1* (1.08 mg), *Fraction 2* (0.95 mg), *Fraction 3* (1.77 mg), *Fraction 4* (1.05 mg), *Fraction 5* (0.95 mg), *Fraction 6* (1.33g), *Fraction 7* (1.00 mg), *Fraction 8* (0.55 mg), *Fraction 9* (0.69 mg), *Fraction 10* (1.20 mg), *Fraction 11* (0.51 mg), *Fraction 12* (0.29 mg), *Fraction 13* (2.11 mg) and *Fraction 14* (0.85 mg)) were dissolved separately in 40 mL Milli-Q water. Following a 100-fold dilution with Milli-Q water, each of the stock solutions was stored at -20 °C until used. Given that, based on ESI-MS analysis, some of the fractions had similar compositions, *vide infra*, these were pooled to give four new fractions, designated as: *Fr1* (*Fraction 1*), *Fr2* (*Fractions 2-5*), *Fr3* (*Fractions 6-10*), *Fr4* (*Fractions 11-14*).

Mass spectrometry

All CaR-ESI-MS measurements were carried out in negative ion mode using a Synapt G2 ESI quadrupole-ion mobility separation-time-of-flight (Q-IMS-TOF) mass spectrometer (Waters, Manchester, UK), equipped with a nanoflow ESI (nanoESI) source. NanoESI tips were produced in-house from borosilicate capillaries (1.0 mm o.d., 0.78 mm i.d.) pulled to ~5 µm outer-diameter using a P-1000 micropipette puller (Sutter Instruments, Novato, CA). To perform nanoESI, a platinum wire was inserted into the nanoESI tip and a voltage of -1.0 kV was applied. A Cone voltage of 25 V was used and the source block temperature was maintained at 50 ºC. For the CaR-ESI-MS measurements, a Trap voltage of 5 V, and Transfer voltage between 10 V and 80 V, was used. Argon was used in the Trap and Transfer ion guides at pressures of 2.22 x 10^{-2} mbar and 3.36 x 10^{-2} mbar, respectively. The helium chamber preceding the traveling wave IMS (TWIMS) device was maintained at 7.72 mbar. The IMS parameters, which were optimized for

Analyst Accepted Manuscript

View Article Online
DOI: 10.1039/C7AN01397C

Published on 27 November 2017. Downloaded by University of Nottingham on 27/11/2017 21:14:28.

each HMO MW, were: 2 mL min^{-1} Trap gas flow rate; 150 to 180 mL min^{-1} helium cell gas flow rate; 50 mL min^{-1} to 90 mL min^{-1} ion mobility gas flow rate; 50 V Trap voltage; 400 m s^{-1} to 1000 m s^{-1} IMS wave velocity; 15 V to 40 V IMS wave height. All IMS measurements were carried out using nitrogen as the mobility gas, at a pressure of 3.41 mbar. Data acquisition and processing were carried out using MassLynx (v4.1). The quantitative affinity measurements were carried out in positive ion mode using a Synapt G2S quadrupole-ion mobility separation-time-of-flight (Q-IMS-TOF) mass spectrometer (Waters UK Ltd., Manchester, UK). Details of the instrumental conditions used and data analysis are given as Supporting Information.

Glycan array screening for binding of BabA

Binding of BabA to a mammalian glycan array was assessed by the Consortium for Functional Glycomics (CFG, Beth Israel Deaconess Medical Center, Harvard Medical School, Boston, MA, USA) using their in-house glycan binding assay protocols and reagents. Binding of BabA to the printed surface of the CFG version 5.2 array, containing 609 synthetic and mammalian glycans, was performed in a 20 mM Tris-Cl (pH 7.4), 300 mM NaCl and 0.05% Tween-20 buffer. Bound BabA was detected with a fluorescein isothiocyanate labelled anti-c-Myc antibody.

Results and discussion

A two-step approach was used to identify HMO ligands, present in the fractions, for the two lectins (Figure 1). First, each fraction was analyzed by ESI-IMS-MS/MS in order to identify, to the extent possible, the HMOs present. This was accomplished by comparing the MWs, IMS-ATs and CID fingerprints of ions detected from the fractions and the MWs of the most abundant oligosaccharidess found in human milk[13-15] and IMS-ATs and CID fingerprints recently reported for a library of thirty-one purified HMOs.[34] In cases where appropriate HMO standards were not available, possible HMO structures were suggested based on the CID fragmentation data and the

Analyst Accepted Manuscript

View Article Online
DOI: 10.1039/C7AN01397C

Published on 27 November 2017. Downloaded by University of Nottingham on 27/11/2017 21:14:28.

structures known to be present in human milk. To our knowledge, the present work represents the first demonstration of using IMS-ATs and CID fingerprinting to identify HMOs in mixtures extracted from human milk. Following the characterization of the fractions, they were screened against the lectin using CaR-ESI-MS and ligands identified from a comparison of the MWs, IMS ATs and CID fingerprints of the released and free HMOs.

a. ESI-MS analysis of HMO fractions *Fr1 – Fr4*

Shown in Figures 2 and S1-S5 (Supporting Information) are representative ESI mass spectra and IMS arrival time distributions (ATDs), acquired in negative ion mode, for aqueous solutions of each of the four fractions. Singly and doubly deprotonated ions corresponding to twelve HMO MWs (633.21 Da, 837.25 Da, 853.31 Da, 999.36 Da, 1056.39 Da, 1072.38 Da, 1202.30 Da, 1218.44 Da, 1364.50 Da, 1510.32 Da, 1583.46 Da and 1729.64 Da) were identified in *Fr1*, six MWs (691.25 Da, 707.25 Da, 837.25 Da, 853.31 Da, 999.36 Da and 1218.44 Da) in *Fr2*, two in *Fr3* (488.17 Da and 707.25 Da), as well as lactose, and seven in *Fr4* (633.21 Da, 836.20 Da, 998.34 Da, 1289.44 Da, 1509.54 Da, 1655.59 Da and 1800.63 Da). It should be noted that some of the HMO MWs were detected in multiple fractions. The monosaccharide compositions of the twenty-one different HMO MWs, which contain between three and ten monosaccharide units, were identified (Table 1). Fourteen of the MWs correspond to neutral HMOs (twelve of these are fucosylated), with the remaining seven corresponding to acidic HMOs (three are fucosylated).

The deprotonated ions (singly or doubly charged) associated with each HMO MW were then subjected to IMS analysis and CID fingerprinting and the results compared to those measured for **HMO1-HMO31**.[34] As an example, the IMS and CID data acquired for the HMOs in *Fr2* are shown in Figure 2; the corresponding results obtained for *Fr1*, *Fr3* and *Fr4* are shown in Figures S2-S5 (Supporting Information). Inspection of Figure 2 reveals that the IMS-ATDs

Analyst Accepted Manuscript

View Article Online
DOI: 10.1039/C7AN01397C

Published on 27 November 2017. Downloaded by University of Nottingham on 27/11/2017 21:14:28.

measured for deprotonated ions corresponding to HMO MWs of 691.25 Da (m/z 690.25), 837.25 Da (m/z 836.25) and 853.31 Da (m/z 852.31) exhibit single features, with ATs of 6.17 ms (Figure 2b), 12.32 ms (Figure 2d) and 12.43 ms (Figure 2e), respectively. For the MWs 707.25 Da (m/z 707.25), 999.36 Da (m/z 998.36) and 1218.44 Da (m/z 608.22) the IMS-ATDs consisted of two and three features, respectively, with ATs of 10.34 Da and 11.66 Da (for 707.25 Da (m/z 707.25)) and 15.18 ms, 15.29 ms and 16.28 ms (for 999.36 Da (m/z 998.36)), 6.16 ms and 6.71 ms (for 1218.44 Da (m/z 608.22)) (Figures 2c, 2f and 2a, respectively). The IMS-ATD measured for the 853.31 Da HMO (m/z 852.31) has a broad distribution (FWHM 1.2 ms) centred at 12.43 ms, consistent with the presence of multiple isomers (Figure 2e).[34]

Four of the measured MWs (691.25 Da, 707.25 Da, 999.36 Da and 853.31 Da) present in *Fr2* coincide with those of HMOs in the thirty-one component library (**HMO1-HMO31**). Comparison of the IMS-ATDs reveals that the ion corresponding to MW 691.25 Da (m/z 690.25), which has an AT of 6.17 ms, matches that of **HMO30** (Figure 2b). The two features (with ATs of 10.34 ms and 11.66 ms) observed for the ions corresponding to MW 707.25 Da (m/z 706.25) match the IMS-ATs measured for **HMO6** and **HMO7** (Figure 2c). The three partially resolved features (with ATs of 15.18 ms, 15.29 ms and 16.28 ms) measured for the ions with MW 999.36 Da (m/z 998.36) match those of **HMO18**, **HMO19** and **HMO20**, respectively (Figure 2f). Additionally, the CID mass spectrum acquired for deprotonated ions of MW 853.31 Da (m/z 853.31) revealed the presence of unique HMO fragments arising from five different HMOs, C_2 (m/z 325.12) from **HMO9**, $^{0,4}A_2/Z_{3\beta}$ (m/z 288.10) from **HMO10,** $C_2/Z_{3\beta}$ (m/z 364.11) from **HMO11,** C_2/Z_3 (m/z 202.07) from **HMO12** and $^{0,2}A_2–H_2O$ (m/z 263.10) from **HMO13** (Figure 2g)**.**

Analyst Accepted Manuscript

View Article Online
DOI: 10.1039/C7AN01397C

Published on 27 November 2017. Downloaded by University of Nottingham on 27/11/2017 21:14:28.

Following the same approach, the other three fractions were analyzed and the HMOs identified are listed in Table 1. Together, the four fractions are found to contain at least thirty-five different HMOs, corresponding to twenty-one different MWs. The structures of twenty-five HMOs (corresponding to eleven different MWs) were established from the measured IMS-ATs and CID fingerprints and comparison with those of purified HMOs. Eighteen of these are neutral HMOs (of which fourteen are fucosylated) and seven are acidic HMOs. For the other MWs, only monosaccharide compositions could be determined. However, it was possible to suggest HMO structures based on previously identified HMOs having the same monosaccharide compositions.[13,14] In certain cases, it was possible to reduce the number of structures based on an analysis of the fragment ions produced by CID (Figures S6-S15, Supporting Information). For example, CID of deprotonated HMOs with MW 836.25 Da (Hex2HexNAcSia) produced fragment ions at m/z 306.14, m/z 470.14 and m/z 493.15 (Figure S6, Supporting Information), which are indicative of α2→6 linked sialic acid, α-Neu5Ac-(2→6)-β-Gal and α-Neu5Ac-(2→6)-β-GlcNAc, respectively.[39] These data, taken together with the previously identified HMOs with Hex2HexNAcSia composition, suggest the presence of both β- GlcNAc-(1→3)-[α-Neu5Ac-(2→6)]-β-Gal-(1→4)-β-Glc and α-Neu5Ac-(2→6)-β-GlcNAc-(1→3/6)-β-Gal-(1→4)-β-Glc.

b. Screening HMO fractions against hGal-3C

Having established the HMO compositions of *Fr1-Fr4*, each fraction was screened against hGal-3C. Shown in Figure 3a is a representative ESI mass spectrum acquired in negative ion mode for aqueous ammonium acetate solutions (40 mM, pH 6.8) of hGal-3C (15 μM), P_{ref} (5 μM) and *Fr2* (0.05 μg μL^{-1}). Signal corresponding to hGal-3C bound to HMOs with five different MWs (691.25 Da (m/z 690.29), 707.25 Da (m/z 706.24), 837.25 Da (m/z 836.20), 853.31 Da (m/z 852.30) and 999.36 Da (m/z 998.37)) was detected. The absence of signal corresponding to

Analyst Accepted Manuscript

View Article Online
DOI: 10.1039/C7AN01397C

Published on 27 November 2017. Downloaded by University of Nottingham on 27/11/2017 21:14:28.

HMO-bound P_{ref} ions indicates that non-specific HMO-hGal-3C binding during the ESI process was negligible.[26] From the MWs of the detected hGal-3C-HMO complexes it was possible to identify only one of the HMO ligands (**HMO30**, MW 691.25 Da); each of the other detected MWs could, in principle, correspond to multiple HMOs.

To identify the other HMO ligands, the (hGal-3C + HMO) complexes at the -7 charge state, the most abundant charge state detected, were isolated using the quadrupole mass filter (set to pass a range (~200 m/z) of ions), and subjected to collisional activation in the Trap region. The selected Trap voltage (40 V) allowed for the efficient release of the HMOs from hGal-3C without causing significant secondary fragmentation. Signal corresponding to deprotonated HMO ions (as well as chloride adducts) of the five different MWs were detected (Figure 3b). From comparison of the IMS-ATDs and CID fingerprints of the released HMO ions with available data for purified HMOs of the same MW, nine HMO ligands (**HMO6**, **HMO7**, **HMO9**, **HMO10**, **HMO11**, **HMO12**, **HMO13**, **HMO18** and **HMO30**) were positively identified (Figure 3c-3h), in addition to the HMO with MW 837.25 Da.

Similar analysis of the CaR-ESI-MS data acquired for the other three fractions with hGal-3C was performed (Figures S16-S18, Supporting information). Taken together, the CaR-ESI-MS data obtained for the four fractions revealed HMO ligands corresponding to seventeen different MWs (Table 2). The structures of twenty-one HMO ligands (corresponding to eleven different MWs) were established from IMS-ATs and CID fingerprints. For the remaining six MWs only monosaccharide composition (and their corresponding putative structures) could be determined (Table 2). Notably, all of the twenty-one HMO ligands for which the structures were conclusively identified (**HMO1**, **HMO3**, **HMO6, HMO7, HMO9 - HMO17, HMO18**,

Analyst Accepted Manuscript

View Article Online
DOI: 10.1039/C7AN01397C

Published on 27 November 2017. Downloaded by University of Nottingham on 27/11/2017 21:14:28.

HMO21, **HMO22, HMO25 - HMO27, HMO30** and **HMO31**) were previously shown to bind to hGal-3C with measurable affinity.[21]

c. Screening HMO fractions against BabA

Having established that the CaR-ESI-MS assay can be applied to HMO fractions, the assay was used to screen *Fr1 – Fr4* against a truncated form of BabA, corresponding to the extracellular region of the adhesin. Shown in Figure 4a is a representative ESI mass spectrum acquired in negative ion mode for an aqueous ammonium acetate solution (40 mM, pH 6.8) of BabA (5 μM) and *Fr2* (0.05 μg μL^{-1}). Signal corresponding to both free and HMO-bound BabA ions, at charge states -11 to -14, were detected. Unlike with hGal-3C, the individual (BabA + HMO) complex ions were not well resolved, making it impossible to determine the MWs of the bound HMOs. Collisional activation of the (BabA + HMO) complexes, at the -13 charge state, resulted in the appearance of ions corresponding to five different HMO MWs (Figure 4b). Based on the IMS-ATs and CID fingerprints of the released ions, eleven different HMO ligands were positively identified **- HMO6**, **HMO7**, **HMO9-HMO13, HMO18-HMO20** and **HMO30** (Figures 4c-4h), plus the HMO with MW 837.25 Da. The other three fractions were screened in a similar fashion and the results are shown in Figures S19-S21 (Supporting Information).

In total, CaR-ESI-MS screening identified HMO ligands of BabA at nine different MWs (Table 3). The specific structures of nineteen of these (corresponding to seven different MWs) were identified (Table 3). Thirteen of the HMOs are neutral (**HMO1, HMO2, HMO6, HMO7, HMO9, HMO10, HMO11, HMO12, HMO13, HMO18, HMO19, HMO20, HMO30**), with two of these being non-fucosylated (**HMO6** and **HMO7**). Notably, BabA is also found to recognize the acidic HMOs (**HMO3**, **HMO4** and **HMO14 - HMO17**). The broad specificity of BabA for HMOs, both neutral and acidic, is, at least in part, consistent with the findings of

Analyst Accepted Manuscript

View Article Online
DOI: 10.1039/C7AN01397C

Published on 27 November 2017. Downloaded by University of Nottingham on 27/11/2017 21:14:28.

previous studies on glycan binding. BabA was shown previously to bind to the blood group O determinants on type 1 core chains, i.e., Lewis b antigen (α-L-Fuc-(1→2)-β-D-Gal-(1→3)-[α-L-Fuc-(1→4)]-β-D-GlcNAc-) and the crystal structure of BabA with **HMO18**, which contains this motif (α-L-Fuc-(1→2)-β-D-Gal-(1→3)-[α-L-Fuc-(1→4)]-β-D-GlcNAc-(1→3)-β-D-Gal(1→4)-β-D-Glc) was reported.[40] BabA also recognizes the H type 1 determinant (α-L-Fuc-(1→2)-β-D-Gal-(1→3)-β-D-GlcNAc-), which is found in **HMO9** (α-L-Fuc(1→2)-β-D-Gal(1→3)-β-D-GlcNAc(1→3)-β-D-Gal(1→4)-β-D-Glc).[35,36,40,41] Results obtained by screening BabA against a mammalian glycan array (Consortium for Functional Glycomics, array version 5.2, Figure S22, Supporting Information) also suggest that the acidic HMOs **HMO3** and **HMO4** and the non-fucosylated HMOs **HMO6** and **HMO7** are BabA ligands.

The ability of BabA to bind to both fucosylated and non-fucosylated neutral, as well as acidic, HMOs is curious. The protein, which is mainly composed of α helices, is known to possess a shallow binding site at the tip of a region called the 'crown', consisting of four antiparallel β-strands located on the head region. Analysis of the reported crystal structure of BabA (*H. pylori* strain J99; 4ZH7.pdb) with **HMO18** suggests that Fuc1 is critical for binding as it participates in a network of hydrogen bonds with C189, G191, N194 and T246. Gal5, GlcNAc3 and Fuc4 also participate in one or more intermolecular or water-mediated hydrogen bonds.[40] Based on this analysis, it is difficult to rationalize the binding of the HMOs that lack the critical elements of the Lewis b hexasaccharide structure, in particular the non-fucosylated and acidic HMOs, at the known binding site. This raises the question of whether BabA possesses an additional glycan binding site (or sites) that recognize HMOs. To test this possibility, ESI-MS binding measurements were performed on solutions of BabA with **HMO18** and either an acidic (**HMO3**) or non-fucosylated HMO (**HMO6**), in varying concentrations. Notably, the mass

Analyst Accepted Manuscript

View Article Online
DOI: 10.1039/C7AN01397C

Published on 27 November 2017. Downloaded by University of Nottingham on 27/11/2017 21:14:28.

spectra showed evidence of ternary complexes (BabA + **HMO18** + **HMO3**) (Figure S23) and (BabA + **HMO18** + **HMO6**) (Figure S24, Supporting Information). These results indicate that BabA possesses at least one additional glycan binding site, distinct from that occupied by **HMO18**, which can recognize HMOs. However, follow-up studies are required to establish the number and nature of the newly identified HMO binding site(s).

The aforementioned binding data also suggest that the affinities of the **HMO3** and **HMO6** for BabA are lower than that of **HMO18**. To establish this more conclusively, ESI-MS affinity measurements were performed on solutions of BabA and individual HMOs (**HMO1**, **HMO2**, **HMO3, HMO4, HMO6**, **HMO7** and **HMO9**, as well as **HMO18**). Representative ESI mass spectra are shown in Figures S25 and S26 (Supporting Information). From an analysis of the relative abundances of the free and HMO-bound BabA ions, the affinities of **HMO9** and **HMO18**, which presumably bind predominantly at the previously identified binding site, were measured to be ~10^4 M^{-1}. This value agrees, within a factor of 3, with a value reported previously for **HMO18**.[40] The affinities of the other HMOs tested are somewhat lower, between $1x10^3$ M^{-1} and $4x10^3$ M^{-1} (Table S2, Supporting Information).

Conclusions

This work describes the first application of CaR-ESI-MS for screening natural libraries of HMOs, derived from pooled breast milk, against target proteins. A total of twenty-one different HMO MWs were identified in the four fractions used in the present study. The structures of twenty-five HMOs, corresponding to eleven different MWs, were identified based on their IMS-ATs and CID fingerprints. To our knowledge, this is the first report describing the use of IMS-ATs and CID fingerprinting for identifying HMOs in mixtures. For the other MWs, monosaccharide composition and, in some cases, possible structures were established. Implementation of the assay was demonstrated using hGal-3C, which served as a model HMO binding lectin. The assay

Analyst Accepted Manuscript

View Article Online
DOI: 10.1039/C7AN01397C

Published on 27 November 2017. Downloaded by University of Nottingham on 27/11/2017 21:14:28.

revealed HMO ligands corresponding to seventeen different MWs. From a comparison of IMS-ATs and CID fingerprints measured for the released HMO ligands and for a library of thirty-one pure HMOs, the structures of twenty-one HMO ligands were identified. Each of these glycans was previously shown to bind to hGal-3C. The presence of HMO ligands at six other MWs was also ascertained; however, the exact structures of these ligands could not be conclusively established. Application of the assay to BabA revealed nineteen specific HMO structures that are recognized by the protein and HMO ligands at two other MWs. Notably, it is found that BabA exhibits broad specificity for HMOs, and can bind to both neutral HMOs, including non-fucosylated ones, and acidic HMOs. The results of competitive binding experiments revealed that, at least, some HMOs can interact with BabA at a previously unknown binding site (or sites); however, the number and nature of the HMO binding site(s) were not established. Finally, the results of quantitative binding measurements performed on eight purified HMOs for BabA produced affinities that are in the 10^3 M^{-1} to 10^4 M^{-1} range.

Acknowledgement

The authors acknowledge the Natural Sciences and Engineering Research Council of Canada and the Alberta Glycomics Centre for funding and Prof. C. Cairo (University of Alberta) for generously providing protein used in this study. We thank Paul R. Gellert and Ross Overman (both AstraZeneca R&D) for their advice and support. Part of this research was funded by the Engineering and Physical Sciences Research Council (EPSRC; grant EP/I01375X/1) and AstraZeneca R&D (NH and FHF).

Analyst Accepted Manuscript

View Article Online
DOI: 10.1039/C7AN01397C

Published on 27 November 2017. Downloaded by University of Nottingham on 27/11/2017 21:14:28.

References

1. F. Lara-Villoslada, M. Olivares, S. Sierra, J.M. Rodríguez, J. Boza, J. Xaus, *Br J Nutr.*, 2007, **98**, S96-S100.
2. O. Ballard, A.L. Morrow, *Pediatr Clin North Am.*, 2013, **60**, 49-74.
3. R. Martín, S. Langa, C. Reviriego, E. Jimínez, M.L. Marín, J. Xaus, L. Fernández, J.M. Rodríguez, *J Pediatr.*, 2003, **143**, 754-758.
4. C. Kunz, S. Rudloff, W. Baier, N. Klein, S. Strobel, *Annu Rev Nutr.*, 2000, **20**, 699-722.
5. A. Kulinich, L. Liu, *Carbohydr Res.*, 2016, **432**, 62-70.
6. J.T. Smilowitz, C.B. Lebrilla, D.A. Mills, J.B. German, S.L. Freeman, *Annu. Rev. Nutr.*, 2014, **34**, 143-169.
7. L. Bode, *Glycobiology*, 2012, **22**, 1147-1162.
8. E. Van Hoffen, B. Ruiter, J. Faber, L. M'Rabet, E.F. Knol, B. Stahl, S. Arslanoglu, G. Moro, G. Boehm, J. Garssen, *J. Allergy*, 2009, **64**, 484-487.
9. R.E. Ward, M. Ninonuevo, D.A. Mills, C.B. Lebrilla, J.B. German, *Appl Environ Microb.*, 2006, **72**, 4497-4499.
10. S.J. Langlands, M.J. Hopkins, N. Coleman, J.H. Cummings, *Gut*, 2004, **53**, 1610-1616.
11. J.B. German, S.L. Freeman, C.B. Lebrilla, D.A. Mills, *Nestle Nutr Workshop Ser Pediatr Program*, 2008, **62**, 205-218.
12. C. Kunz, S. Rudloff, W. Baier. N. Klein. S. Strobel, *Annu Rev of Nutr.*, 2000, **20**, 699-722.
13. S. Wu, N. Tao, J.B. German, R. Grimm, C. Lebrilla, *J. Proteome Res.*, 2010, **9**, 4138-4151.
14. S. Wu, R. Grimm, J.B. German, C.B. Lebrilla, *J. Proteome Res.*, 2011, **10**, 856-868.
15. B. Finke, B. Stahl, A. Pfenninger, M. Karas, H. Daniel, G. Sawatzki, *Anal. Chem.*, 1999, **71**, 3755-3762.

Analyst Accepted Manuscript

View Article Online
DOI: 10.1039/C7AN01397C

Published on 27 November 2017. Downloaded by University of Nottingham on 27/11/2017 21:14:28.

16. B. Stahl, S. Thurl, J. Zeng, M. Karas, F. Hillenkamp, M. Steup, G. Sawatzki, *Anal Biochem.*, 1994, **223**, 218-26.

17. B. Domon, C. Costello, *Glycoconj. J.*, 1988, **5**, 397-409.

18. S. Xuezheng, Y. Lasanajak, B. Xia, J. Heimburg-Molinaro, J.R. Jeanne M. Rhea, H. Hong Ju, C. Zhao, R.J. Molinaro, R.D. Cummings, D.F. Smith, *Nat. Methods*, 2011, **8**, 85-90.

19. A.J. Noll, J.P. Gourdine, Y. Yu, Y. Lasanajak, D.F. Smith, R.D. Cummings, *Glycobiology*, 2016, **26**, 655-669.

20. A.J. Noll, Y. Yu, Y. Lasanajak, G. Duska-McEwen, R.H. Buck, D.F. Smith, R.D. Cummings, *Biochem. J.*, 2016, **473**, 1343-1353.

21. K. Shams-Ud-Doha, E.N. Kitova, P. Kitov, Y. St-Pierre, J.S. Klassen, *Anal Chem.*, 2017, **89**,4914-4921.

22. E.N. Kitova, A. El-Hawiet, P.D. Schnier, J.S. Klassen, *J. Am. Soc. Mass Spectrom.*, 2012, **23**, 431-441.

23. H. Lin, E.N. Kitova, J.S. Klassen, *J. Am. Soc. Mass Spectrom.*, 2014, **25**, 104-110.

24. L. Liu, E.N. Kitova, J.S. Klassen, *J. Am. Soc. Mass Spectrom.*, 2011, **22**, 310-318.

25. W. Wang, E.N. Kitova, J.S. Klassen, *Anal. Chem.*, 2003, **75**, 4945-4955.

26. J. Sun, E.N. Kitova, W. Wang, J.S. Klassen, *Anal. Chem.*, 2006, **78**, 3010-3018.

27. A. El-Hawiet, G.K. Shoemaker, R. Daneshfar, E.N. Kitova, J.S. Klassen, *Anal. Chem.*, 2011, **84**, 50-58.

28. A.C. Leney, X. Fan, E.N. Kitova, J.S. Klassen, *Anal. Chem.*, 2014, **86**, 5271-5277.

29. A. El-Hawiet, E.N. Kitova, J.S. Klassen, *Anal. Chem.*, 2013, **85**, 7637-7644.

30. Y. Zhang, L. Liu, R. Daneshfar, E.N. Kitova, C. Li, F. Jia, C.W. Cairo, J.S. Klassen, J.S. *Anal. Chem.*, 2012, **84**, 7618-7621.

Analyst Accepted Manuscript

View Article Online
DOI: 10.1039/C7AN01397C

Published on 27 November 2017. Downloaded by University of Nottingham on 27/11/2017 21:14:28.

31. L. Han, E.N. Kitova, M. Tan, X. Jiang, J.S. Klassen, *J. Am. Chem. Soc.*, 2014, **25**, 111-119.

32. L. Han, M. Tan, M. Xia, E.N. Kitova, X. Jiang, J.S. Klassen, *J. Am. Chem. Soc.*, 2014, **136**, 12631-12637.

33. E.N. Kitova, A. El-Hawiet, J.S. Klassen, *J. Am. Soc. Mass Spectrom.*, 2014, **25**, 1908-1916.

34. A. El-Hawiet, Y. Chen, K. Shams-Ud-Doha, E.N. Kitova, Y. St-Pierre, J.S. Klassen, *Anal. Chem.*, 2017, **89**, 8713–8722.

35. B. Thomas, P. Falk, K.A. Roth, G. Larson, S. Normark, *Science*, 1993, **262**,1892-1895.

36. M. Aspholm-Hurtig, G. Dailide, M. Lahmann, A. Kalia, D. Ilver, N. Roche, S. Vikström, R. Sjöström, S. Lindén, A. Bäckström, C. Lundberg, A. Arnqvist, J. Mahdavi, U.J. Nilsson, B. Velapatiño, R.H. Gilman, M. Gerhard, T. Alarcon, M. López-Brea, T. Nakazawa, J.G. Fox, P. Correa, M.G. Dominguez-Bello, G.I. Perez-Perez, M.J. Blaser, S. Normark, I. Carlstedt, S. Oscarson, S. Teneberg, D.E. Berg, T. Borén, *Science*, 2004, **305**, 519-22.

37. A.R. Pacheco, D. Barile, M.A. Underwood, D.A. Mills, *Annu. Rev. Anim. Biosci.*, 2015, **3**, 419-45.

38. N. Hage, J.G. Renshaw, G.S. Winkler, P. Gellert, S. Stolnik, F. Falcone, *Protein Expr. Purif.*, 2015, **106**, 25-30.

39. S.F. Wheeler, D.J. Harvey, *Anal. Chem.*, 2000, **72**, 5027-5039.

40. N.Hage, T. Howard, C. Phillips, C. Brassington, R.Overman, J. Debreczeni, P. Gellert, S. Stolnik, G.S.Winkler, F.H. Falcone, *Sci. Adv.*, 2015, **1**, e1500315.

41. D. Keilberg, K.M. Ottemann, *Environ Microbiol.*, 2016, **18**, 791-806.

Analyst Accepted Manuscript

View Article Online
DOI: 10.1039/C7AN01397C

Published on 22 November 2017. Downloaded by University of Nottingham on 27/11/2017 21:14:28.

Table 1. MW and monosaccharide composition (Hex ≡ Glc or Gal; HexNAc ≡ GlcNAc; Fuc ≡ fucose and Sia ≡ sialic acid) of HMOs identified from ESI-MS analysis of aqueous solutions of *Fr1 – Fr4.* The identity of specific HMO structures was based on a comparison of IMS-ATs and CID fingerprints of deprotonated ions produced from *Fr1 – Fr4* and those of **HMO1** – **HMO31**.

Fraction	Theoretical MW	Monosaccharide composition	Confirmed/Putative HMO Structures
Fr1	633.21	Hex2Sia	α-D-Neu5Ac-(2→3)-β-D-Gal-(1→4)-β-D-Glc (**HMO3**) α-D-Neu5Ac-(2→6)-β-D-Gal-(1→4)-β-D-Glc (**HMO4**)
	837.25	Hex2HexNAcFuc2	α-L-Fuc-(1→3/4)-β-D-GlcNAc-(1→3/6)-[α-L-Fuc-(1→2/3)]-β-D-Gal-(1→4)-β-D-Glc [a]
	853.31	Hex3HexNAcFuc	α-L-Fuc-(1→2)-β-D-Gal-(1→3)-β-D-GlcNAc-(1→3)-β-D-Gal-(1→4)-β-D-Glc (**HMO9**) β-D-Gal-(1→3)-[α-L-Fuc-(1→4)]-β-D-GlcNAc-(1→3)-β-D-Gal-(1→4)-β-D-Glc (**HMO10**) β-D-Gal-(1→4)-[α-L-Fuc-(1→3)]-β-D-GlcNAc-(1→3)-β-D-Gal-(1→4)-β-D-Glc (**HMO11**) β-D-Gal-(1→3)-β-D-GlcNAc-(1→3)-β-D-Gal-(1→4)-[α-L-Fuc-(1→3)]-β-D-Glc (**HMO12**) β-D-Gal-(1→4)-β-D-GlcNAc-(1→3)-β-D-Gal-(1→4)[α-L-Fuc-(1→3)]-β-D-Glc (**HMO13**)
	999.36	Hex3HexNAcFuc2	α-L-Fuc-(1→2)-β-D-Gal-(1→3)-[α-L-Fuc-(1→4)]-β-D-GlcNAc-(1→3)-β-D-Gal-(1→4)-β-D-Glc (**HMO18**) β-D-Gal-(1→3)-[α-L-Fuc-(1→4)]-β-D-GlcNAc-(1→3)-β-D-Gal-(1→4)-[α-L-Fuc-(1→3)]-β-D-Glc (**HMO19**) β-D-Gal-(1→4)-[α-L-Fuc-(1→3)]-β-D-GlcNAc-(1→3)-β-D-Gal-(1→4)-[α- L-Fuc-(1→3)]-β-D-Glc (**HMO20**)
	1056.39	Hex3HexNAc2Fuc	α-D-GalNAc-(1→3)-[α-L-Fuc-(1→2)]-β-D-Gal-(1→3)-β-GlcNAc(1→3)-β-D-Gal(1→4)-β-D-Glc (**HMO31**)
	1072.38	Hex4HexNAc2	β-D-Gal-(1→4)-β-D-GlcNAc-(1→3)-β-

Analyst Accepted Manuscript

View Article Online
DOI: 10.1039/C7AN01397C

Published on 27 November 2017. Downloaded by University of Nottingham on 27/11/2017 21:14:28.

		D-Gal-(1→4)-β-D-GlcNAc-(1→3)-β-D-Gal-(1→4)-β-D-Glc (**HMO21**) β-D-Gal-(1→4)-β-D-GlcNAc-(1→6)-[β-D-Gal-(1→4)-β-D-GlcNAc-(1→3)]-β-D-Glc-(1→4)-Glc (**HMO22**)
1202.30	Hex3HexNAc2Fuc2	β-D-GlcNAc-(1→3/4)-[L-Fuc-(1→2)]-β-D-Gal-(1→3)-[L-Fuc-(1→4)]-β-D-GlcNAc-(1→3/6)-β-D-Gal-(1→4)-β-D-Glc [a]
1218.44	Hex4HexNAc2Fuc	β-D-Gal-(1→3/4)-β-D-GlcNAc-(1→3/6)-β-D-Gal-(1→3/4)-[L-Fuc-(1→3/4)]-β-D-GlcNAc-(1→3/6)-β-D-Gal-(1→4)-β-D-Glc [a]
1364.50	Hex4HexNAc2Fuc2	β-D-Gal-(1→4)-[α-L-Fuc-(1→3)]-β-D-GlcNAc-(1→6)-[α-L-Fuc-(1→2)-β-D-Gal-(1→3)-β-D-GlcNAc-(1→3)]-β-D-Gal-(1→4)-β-D-Glc (**HMO26**) β-D-Gal-(1→3)-[α-L-Fuc-(1→4)]-β-D-GlcNAc-(1→3)-β-D-Gal-(1→4)-[α-L-Fuc-(1→3)]-β-D-GlcNAc-(1→3)]-β-D-Gal-(1→4)-β-D-Glc (**HMO27**)
1510.32	Hex4HexNAc2Fuc3	α-L-Fuc-(1→2)-β-D-Gal-(1→3)-[α-L-Fuc-(1→4)]-β-D-GlcNAc-(1→3)-[β-D-Gal-(1→4)-[α-L-Fuc-(1→3)]-β-D-GlcNAc]-β-D-Gal-(1→4)-β-D-Glc [a]
1583.46	Hex5HexNAc3Fuc	β-D-Gal-(1→4)-β-D-GlcNAc-(1→3)-β-D-Gal-(1→4)-[α-L-Fuc-(1→3)]-β-D-GlcNAc-(1→6)-[β-D-Gal-(1→3)-β-D-GlcNAc-(1→3)]-β-D-Gal-(1→4)-β-D-Glc [a] β-D-Gal-(1→3)-β-D-GlcNAc-(1→3)-β-D-Gal-(1→4)-[α-L-Fuc-(1→3)]-β-D-GlcNAc-(1→6)-[β-D-Gal-(1→3)-β-D-GlcNAc-(1→3)]-β-D-Gal-(1→4)-β-D-Glc [a]
1729.64	Hex5HexNAc3Fuc2	β-D-Gal-(1→4)-[α-L-Fuc-(1→3)]-β-D-GlcNAc-(1→3)-β-D-Gal-(1→4)-[α-L-Fuc-(1→3)]-β-D-GlcNAc-(1→6)-[β-D-Gal-(1→3)-β-D-GlcNAc]-β-D-Gal-(1→4)-β-D-Glc [a] β-D-Gal-(1→3)-[α-L-Fuc-(1→4)]-β-D-GlcNAc-(1→3)-β-D-Gal-(1→4)-[α-L-Fuc-(1→3)]-β-D-GlcNAc-(1→6)-[β-D-

Analyst Accepted Manuscript

View Article Online
DOI: 10.1039/C7AN01397C

Published on 27 November 2017. Downloaded by University of Nottingham on 27/11/2017 21:14:28.

			Gal-(1→4)-β-D-GlcNAc-(1→3)]-β-D-Gal-(1→4)-β-D-Glc [a] β-D-Gal-(1→4)-β-D-GlcNAc-(1→3)-β-D-Gal-(1→4)-[α-L-Fuc-(1→3)]-β-D-GlcNAc-(1→6)-[β-D-Gal-(1→3)-[α-L-Fuc-(1→4)]-β-D-GlcNAc-(1→3)]-β-D-Gal-(1→4)-β-D-Glc [a] β-D-Gal-(1→3)-β-D-GlcNAc-(1→3)-β-D-Gal-(1→4)-[α-L-Fuc-(1→3)]-β-D-GlcNAc-(1→6)-[β-D-Gal-(1→4)-[α-L-Fuc-(1→3)]-β-D-GlcNAc-(1→3)]-β-D-Gal-(1→4)-β-D-Glc [a]
Fr2	691.25	Hex2HexNAcFuc	α-D-GalNAc-(1→3)-[α-L-Fuc-(1→2)]-β-D-Gal-(1→4)-β-D-Glc (**HMO30**)
	707.25	Hex3HexNAc	β-D-Gal-(1→3)-β-D-GlcNAc-(1→3)-β-D-Gal-(1→4)-β-D-Glc (**HMO6**) β-D-Gal-(1→4)-β-D-GlcNAc-(1→3)-β-D-Gal-(1→4)-β-D-Glc (**HMO7**)
	837.25	Hex2HexNAcFuc2	β-D-GlcNAc-(1→3)-[α-D-Neu5Ac-(2→6)]-β-D-Gal-(1→4)-β-D-Glc[a] α-D-Neu5Ac-(2→6)-β-D-GlcNAc-(1→3/6)-β-D-Gal-(1→4)-β-D-Glc[a]
	853.31	Hex3HexNAcFuc	α-L-Fuc-(1→2)-β-D-Gal-(1→3)-β-D-GlcNAc-(1→3)-β-D-Gal-(1→4)-β-D-Glc (**HMO9**) β-D-Gal-(1→3)-[α-L-Fuc-(1→4)]-β-D-GlcNAc-(1→3)-β-D-Gal-(1→4)-β-D-Glc (**HMO10**) β-D-Gal-(1→4)-[α-L-Fuc-(1→3)]-β-D-GlcNAc-(1→3)-β-D-Gal-(1→4)-β-D-Glc (**HMO11**) β-D-Gal-(1→3)-β-D-GlcNAc-(1→3)-β-D-Gal-(1→4)-[α-L-Fuc-(1→3)]-β-D-Glc (**HMO12**) β-D-Gal-(1→4)-β-D-GlcNAc-(1→3)-β-D-Gal-(1→4)[α-L-Fuc-(1→3)]-β-D-Glc (**HMO13**)
	999.36	Hex3HexNAcFuc2	α-L-Fuc-(1→2)-β-D-Gal-(1→3)-[α-L-Fuc-(1→4)]-β-D-GlcNAc-(1→3)-β-D-Gal-(1→4)-β-D-Glc (**HMO18**) β-D-Gal-(1→3)-[α-L-Fuc-(1→4)]-β-D-GlcNAc-(1→3)-β-D-Gal-(1→4)-[α-L-Fuc-(1→3)]-β-D-Glc (**HMO19**) β-D-Gal-(1→4)-[α-L-Fuc-(1→3)]-β-D-GlcNAc-(1→3)-β-D-Gal-(1→4)-[α- L-

Analyst Accepted Manuscript

View Article Online
DOI: 10.1039/C7AN01397C

Published on 27 November 2017. Downloaded by University of Nottingham on 27/11/2017 21:14:28.

			Fuc-(1→3)]-β-D-Glc (**HMO20**)
	1218.44	Hex4HexNAc2Fuc	β-D-Gal-(1→3/4)-β-D-GlcNAc (1→3/6)-β-D-Gal-(1→3/4)-[L-Fuc-(1→3/4)]-β-D-GlcNAc-(1→3/6)-β-D-Gal-(1→4)-β-D-Glc
Fr3	342.31	Hex2	β-D-Gal-(1→4)-β-D-Glc (**Lactose**)
	488.17	Hex2Fuc	α-L-Fuc-(1→2)-β-D-Gal-(1→4)-β-D-Glc (**HMO1**) β-D-Gal-(1→4)-[α-L-Fuc-(1→3)]-β-D-Glc (**HMO2**)
	707.25	Hex3HexNAc	β-D-Gal-(1→3)-β-D-GlcNAc-(1→3)-β-D-Gal-(1→4)-β-D-Glc (**HMO6**) β-D-Gal-(1→4)-β-D-GlcNAc-(1→3)-β-D-Gal-(1→4)-β-D-Glc (**HMO7**)
Fr4	633.21	Hex2Sia	α-D-Neu5Ac-(2→3)-β-D-Gal-(1→4)-β-D-Glc (**HMO3**) α-D-Neu5Ac-(2→6)-β-D-Gal-(1→4)-β-D-Glc (**HMO4**)
	836.20	Hex2HexNAcSia	β-D-GlcNAc-(1→3/4)-[α-D-Neu5Ac-(2→6)]-β-D-Gal-(1→4)-β-D-Glc [a] α-D-Neu5Ac-(2→6)-)-β-D-GlcNAc-(1→3/4)-β-D-Gal-(1→4)-β-D-Glc [a]
	998.34	Hex3HexNAcSia	α-D-Neu5Ac-(2→3)-β-D-Gal-(1→3)-β-D-GlcNAc-(1→3)-β-D-Gal-(1→4)-β-D-Glc (**HMO14**) α-D-Neu5Ac-(2→6)-[β-D-Gal-(1→3)]-β-D-GlcNAc-(1→3)-β-D-Gal-(1→4)- β-D-Glc (**HMO15**) α-D-Neu5Ac-(2→6)-β-D-Gal-(1→4)-β-D-GlcNAc-(1→3)-β-D-Gal-(1→4)-β-D-Glc (**HMO16**) α-D-Neu5Ac-(2→3)-β-D-Gal-(1→4)-β-D-GlcNAc-(1→3)-β-D-Gal-(1→4)-β-D-Glc (**HMO17**)
	1289.44	Hex3HexNAcSia2	α-D-Neu5Ac-(2→3)-β-D-Gal-(1→3)-[α-D-Neu5Ac-(2→6)]-β-D-GlcNAc-(1→3)-β-D-Gal-(1→4)-β-D-Glc (**HMO25**)
	1509.54	Hex4HexNAc2FucSia	Neu5Ac-(2→6)-β-D-Gal-(1→3/6)-β-D-GlcNAc-(1→3/6)-β-D-Gal-(1→3)-[L-Fuc-(1→3/4)]-β-D-GlcNAc-(1→3/6)-β-D-Gal-(1→4)-β-D-Glc [a]

Analyst Accepted Manuscript

View Article Online
DOI: 10.1039/C7AN01397C

Published on 27 November 2017. Downloaded by University of Nottingham on 27/11/2017 21:14:28.

1655.59	Hex4HexNAc2Fuc2Sia	α-D-Neu5Ac-(2→6)-β-D-Gal-(1→4)-β-D-GlcNAc-(1→3)-[α-L-Fuc-(1→2)-β-D-Gal-(1→4)-α-L-Fuc-(1→3)]-β-D-GlcNAc-(1→6)-β-D-Gal-(1→4)-β-D-Glc [a] α-L-Fuc-(1→2)-β-D-Gal-(1→3)-[α-L-Fuc-(1→4)]-β-D-GlcNAc-(1→3)-[α-D-Neu5Ac-(2→6)-β-D-Gal-(1→4)]-β-D-GlcNAc-(1→3)-]-β-D-Gal-(1→4)-β-D-Glc [a]
1800.63	Hex4HexNAc2FucSia2	α-D-Neu5Ac-(2→6)-[α-D-Neu5Ac-(2→6) -β-D-Gal-(1→3)-]-β-D-GlcNAc-(1→4)-[α-L-Fuc-(1→2)-]-β-D-Gal-(1→4)-β-D-GlcNAc-(1→3)-β-D-Gal-(1→4)-β-D-Glc [a]

a. Possible structures based on CID results and identified HMOs reported in references 13 and 14.

Analyst Accepted Manuscript

View Article Online
DOI: 10.1039/C7AN01397C

Published on 27 November 2017. Downloaded by University of Nottingham on 27/11/2017 21:14:28.

Table 2. MW and monosaccharide composition (Hex ≡ Glc or Gal; HexNAc ≡ GlcNAc; Fuc ≡ fucose and Sia ≡ sialic acid) of HMO ligands of hGal-3C identified from *Fr1 – Fr4* using CaR-ESI-MS. The identity of specific HMO structures was based on a comparison of IMS-ATs and CID fingerprints of deprotonated ligand ions released from hGal-3C and those of **HMO1** – **HMO31**.

Measured MW (Da)	Theoretical MW (Da)	Monosaccharide composition	Confirmed/Putative HMO Structures	
488.17	488.17	Hex2Fuc	α-L-Fuc-(1→2)-β-D-Gal-(1→4)-β-D-Glc (**HMO1**)	
633.22	633.21	Hex2Sia	α-D-Neu5Ac-(2→3)-β-D-Gal-(1→4)-β-D-Glc (**HMO3**)	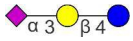
691.29	691.25	Hex2HexNAcFuc	α-D-GalNAc-(1→3)-[α-L-Fuc-(1→2)]-β-D-Gal-(1→4)-β-D-Glc (**HMO30**)	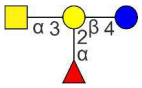
707.24	707.25	Hex3HexNAc	β-D-Gal-(1→3)-β-D-GlcNAc-(1→3)-β-D-Gal-(1→4)-β-D-Glc (**HMO6**) β-D-Gal-(1→4)-β-D-GlcNAc-(1→3)-β-D-Gal-(1→4)-β-D-Glc (**HMO7**)	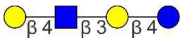 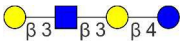
836.20	836.20	Hex2HexNAcSia	β-D-GlcNAc-(1→3/4)-[α-D-Neu5Ac-(2→6)]-β-D-Gal-(1→4)-β-D-Glc [a] α-D-Neu5Ac-(2→6)-β-D-GlcNAc-(1→3/4)-β-D-Gal-(1→4)-β-D-Glc [a]	
837.20	837.25	Hex2HexNAcFuc2	α-L-Fuc-(1→3/4)-β-D-GlcNAc-(1→3/6)-[α-L-Fuc-(1→2/3)]-β-D-Gal-(1→4)-β-D-Glc [a]	
853.30	853.31	Hex3HexNAcFuc	α- L-Fuc-(1→2)-β-D-Gal-(1→3)-β-D-GlcNAc-(1→3)-β-D-Gal-(1→4)-β-D-Glc (**HMO9**)	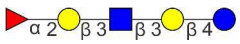

Analyst Accepted Manuscript

View Article Online
DOI: 10.1039/C7AN01397C

Published on 27 November 2017. Downloaded by University of Nottingham on 27/11/2017 21:14:28.

			β-D-Gal-(1→3)-[α-L-Fuc-(1→4)]-β-D-GlcNAc-(1→3)-β-D-Gal-(1→4)-β-D-Glc (**HMO10**)	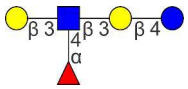
			β-D-Gal-(1→4)-[α-L-Fuc- (1→3)]-β-D-GlcNAc-(1→3)-β-D-Gal-(1→4)-β-D-Glc (**HMO11**)	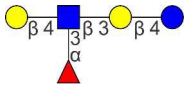
			β-D-Gal-(1→3)-β-D-GlcNAc-(1→3)-β-D-Gal-(1→4)-[α-L-Fuc-(1→3)]-β-D-Glc (**HMO12**)	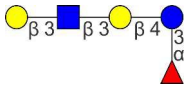
			β-D-Gal-(1→4)-β-D-GlcNAc-(1→3)-β-D-Gal-(1→4)[α-L-Fuc-(1→3)]-β-D-Glc (**HMO13**)	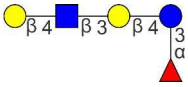
998.33	998.34	Hex3HexNAcSia	α-D-Neu5Ac-(2→3)-β-D-Gal-(1→3)-β-D-GlcNAc-(1→3)-β-D-Gal-(1→4)-β-D-Glc (**HMO14**)	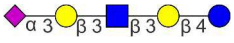
			α-D-Neu5Ac-(2→6)-[β-D-Gal-(1→3)]-β-D-GlcNAc-(1→3)-β-D-Gal-(1→4)- β-D-Glc (**HMO15**)	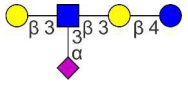
			α-D-Neu5Ac-(2→6)-β-D-Gal-(1→4)-β-D-GlcNAc-(1→3)-β-D-Gal-(1→4)-β-D-Glc (**HMO16**)	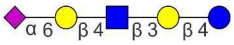
			α-D-Neu5Ac-(2→3)-β-D-Gal-(1→4)-β-D-GlcNAc-(1→3)-β-D-Gal-(1→4)-β-D-Glc (**HMO17**)	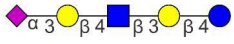
999.37	999.34	Hex3HexNAcFuc2	α-L-Fuc-(1→2)-β-D-Gal-(1→3)-[α-L-Fuc-(1→4)]-β-D-GlcNAc-(1→3)-β-D-Gal-(1→4)-β-D-Glc (**HMO18**)	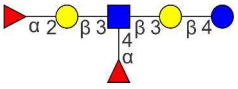
1056.39	1056.39	Hex3HexNAc2Fuc	α-D-GalNAc-(1→3)-[α-L-Fuc-(1→2)]-β-D-Gal-(1→3)-β-GlcNAc(1→3)-	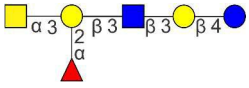

Analyst Accepted Manuscript

View Article Online
DOI: 10.1039/C7AN01397C

Published on 27 November 2017. Downloaded by University of Nottingham on 27/11/2017 21:14:28.

			β-D-Gal(1→4)-β-D-Glc (**HMO31**)	
1072.38	1072.38	Hex4HexNAc2	β-D-Gal-(1→4)-β-D-GlcNAc-(1→3)-β-D-Gal-(1→4)-β-D-GlcNAc-(1→3)-β-D-Gal-(1→4)-β-D-Glc (**HMO21**) β-D-Gal-(1→4)-β-D-GlcNAc-(1→6)-[β-D-Gal-(1→4)-β-D-GlcNAc-(1→3)]-β-D-Glc-(1→4)-Glc (**HMO22**)	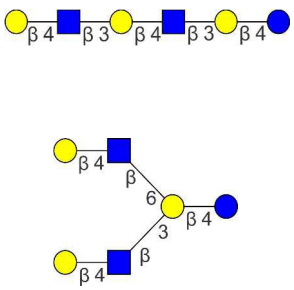
1218.44	1218.44	Hex4HexNAc2Fuc	β-D-Gal-(1→3/4)-β-D-GlcNAc (1→3/6)-β-D-Gal-(1→3/4)-[L-Fuc-(1→3/4)]-β-D-GlcNAc-(1→3/6)-β-D-Gal-(1→4)-β-D-Glc [a]	
1289.43	1289.44	Hex3HexNAcSia2	α-D-Neu5Ac-(2→3)-β-D-Gal-(1→3)-[α-D-Neu5Ac-(2→6)]-β-D-GlcNAc-(1→3)-β-D-Gal-(1→4)-β-D-Glc (**HMO25**)	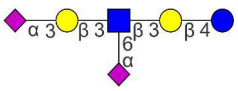
1364.49	1364.50	Hex4HexNAc2Fuc2	β-D-Gal-(1→4)-[α-L-Fuc-(1→3)]-β-D-GlcNAc-(1→6)-[α-L-Fuc-(1→2)-β-D-Gal-(1→3)-β-D-GlcNAc-(1→3)]-β-D-Gal-(1→4)-β-D-Glc (**HMO26**) β-D-Gal-(1→3)-[α-L-Fuc-(1→4)]-β-D-GlcNAc-(1→3)-β-D-Gal-(1→4)-[α-L-Fuc-(1→3)]-β-D-GlcNAc-(1→3)]-β-D-Gal-(1→4)-β-D-Glc (**HMO27**)	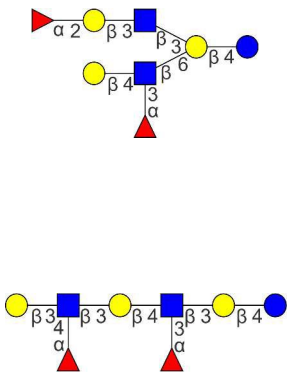
1509.52	1509.54	Hex4HexNAc2FucSia	Neu5Ac-(2→6)-β-D-Gal-(1→3/6)-β-D-GlcNAc-(1→3/6)-β-D-Gal-(1→3)-[L-Fuc-(1→3/4)]-β-D-GlcNAc-(1→3/6)-β-D-Gal-(1→4)-β-D-Glc [a]	

Analyst Accepted Manuscript

View Article Online
DOI: 10.1039/C7AN01397C

Published on 27 November 2017. Downloaded by University of Nottingham on 27/11/2017 21:14:28.

1655.54	1655.59	Hex4HexNAc2Fuc2Sia	α-D-Neu5Ac-(2→6)-β-D-Gal-(1→4)-β-D-GlcNAc-(1→3)-[α-L-Fuc-(1→2)-β-D-Gal-(1→4)-α-L-Fuc-(1→3)]-β-D-GlcNAc-(1→6)-β-D-Gal-(1→4)-β-D-Glc [a] α-L-Fuc-(1→2)-β-D-Gal-(1→3)-[α-L-Fuc-(1→4)]-β-D-GlcNAc-(1→3)-[α-D-Neu5Ac-(2→6)-β-D-Gal-(1→4)]-β-D-GlcNAc-(1→3)-]-β-D-Gal-(1→4)-β-D-Glc [a]
1800.62	1800.63	Hex4HexNAc2FucSia2	α-D-Neu5Ac-(2→6)-[α-D-Neu5Ac-(2→6) -β-D-Gal-(1→3)-]-β-D-GlcNAc-(1→4)-[α-L-Fuc-(1→2)-]-β-D-Gal-(1→4)-β-D-GlcNAc-(1→3)-β-D-Gal-(1→4)-β-D-Glc [a]

a. Possible structures based on CID results and identified HMOs reported in references 13 and 14.

Analyst Accepted Manuscript

View Article Online
DOI: 10.1039/C7AN01397C

Published on 27 November 2017. Downloaded by University of Nottingham on 27/11/2017 21:14:28.

Table 3. HMO ligands of BabA identified from *Fr1 – Fr4* using CaR-ESI-MS. The identity of specific HMO structures was based on a comparison of IMS-ATs and CID fingerprints of deprotonated ligand ions released from hGal-3C and those of **HMO1** – **HMO31**.

Measured MW (Da)	Theoretical MW (Da)	Monosaccharide composition	Confirmed/Putative HMO Structures	
488.13	488.17	Hex2Fuc	α-L-Fuc-(1→2)-β-D-Gal-(1→4)-β-D-Glc **(HMO1)** α-L-Fuc-(1→3)-β-D-Gal-(1→4)-β-D-Glc **(HMO2)**	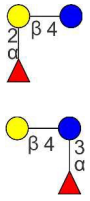
633.23	633.21	Hex2Sia	α-D-Neu5Ac-(2→3)-β-D-Gal-(1→4)-β-D-Glc **(HMO3)** α-D-Neu5Ac-(2→6)-β-D-Gal-(1→4)-β-D-Glc **(HMO4)**	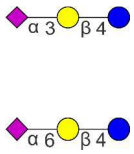
691.29	691.25	Hex2HexNAcFuc	α-D-GalNAc-(1→3)-[α-L-Fuc-(1→2)]-β-D-Gal-(1→4)-β-D-Glc **(HMO30)**	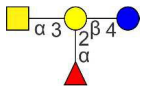
707.25	707.25	Hex3HexNAc	β-D-Gal-(1→3)-β-D-GlcNAc-(1→3)-β-D-Gal-(1→4)-β-D-Glc **(HMO6)** β-D-Gal-(1→4)-β-D-GlcNAc-(1→3)-β-D-Gal-(1→4)-β-D-Glc **(HMO7)**	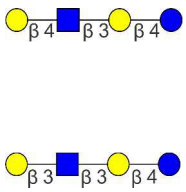
837.20	837.25	Hex2HexNAcFuc2	α-L-Fuc-(1→3/4)-β-D-GlcNAc-(1→3/6)-[α-L-Fuc-(1→2/3)]-β-D-Gal-(1→4)-β-D-Glc [a]	
853.31	853.31	Hex3HexNAcFuc	α- L-Fuc-(1→2)-β-D-Gal-(1→3)-β-D-GlcNAc-(1→3)-β-D-Gal-(1→4)-β-D-Glc **(HMO9)**	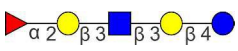

Analyst Accepted Manuscript

View Article Online
DOI: 10.1039/C7AN01397C

Published on 27 November 2017. Downloaded by University of Nottingham on 27/11/2017 21:14:28.

			β-D-Gal-(1→3)-[α-L-Fuc-(1→4)]-β-D-GlcNAc-(1→3)-β-D-Gal-(1→4)-β-D-Glc **(HMO10)**	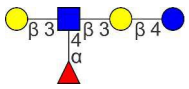
			β-D-Gal-(1→4)-[α-L-Fuc-(1→3)]-β-D-GlcNAc-(1→3)-β-D-Gal-(1→4)-β-D-Glc **(HMO11)**	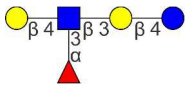
			β-D-Gal-(1→3)-β-D-GlcNAc-(1→3)-β-D-Gal-(1→4)-[α-L-Fuc-(1→3)]-β-D-Glc **(HMO12)**	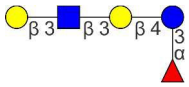
			β-D-Gal-(1→4)-β-D-GlcNAc-(1→3)-β-D-Gal-(1→4)[α-L-Fuc-(1→3)]-β-D-Glc **(HMO13)**	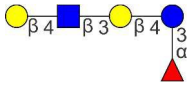
998.33	998.34	Hex3HexNAcSia	α-D-Neu5Ac-(2→3)-β-D-Gal-(1→3)-β-D-GlcNAc-(1→3)-β-D-Gal-(1→4)-β-D-Glc **(HMO14)**	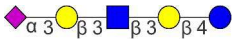
			α-D-Neu5Ac-(2→6)-[β-D-Gal-(1→3)]-β-D-GlcNAc-(1→3)-β-D-Gal-(1→4)- β-D-Glc **(HMO15)**	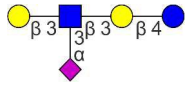
			α-D-Neu5Ac-(2→6)-β-D-Gal-(1→4)-β-D-GlcNAc-(1→3)-β-D-Gal-(1→4)-β-D-Glc **(HMO16)**	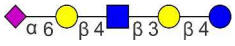
			α-D-Neu5Ac-(2→3)-β-D-Gal-(1→4)-β-D-GlcNAc-(1→3)-β-D-Gal-(1→4)-β-D-Glc **(HMO17)**	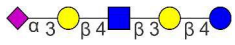
999.38	999.36	Hex3HexNAcFuc2	α-L-Fuc-(1→2)-β-D-Gal-(1→3)-[α-L-Fuc-(1→4)]-β-D-GlcNAc-(1→3)-β-D-Gal-(1→4)-β-D-Glc **(HMO18)**	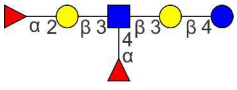

Analyst Accepted Manuscript

View Article Online
DOI: 10.1039/C7AN01397C

Published on 27 November 2017. Downloaded by University of Nottingham on 27/11/2017 21:14:28.

			β-D-Gal-(1→3)-[α-L-Fuc-(1→4)]-β-D-GlcNAc-(1→3)-β-D-Gal-(1→4)-[α-L-Fuc-(1→3)]-β-D-Glc **(HMO19)**	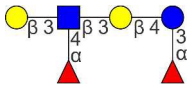
			β-D-Gal-(1→4)-[α-L-Fuc-(1→3)]-β-D-GlcNAc-(1→3)-β-D-Gal-(1→4)-[α- L-Fuc-(1→3)]-β-D-Glc **(HMO20)**	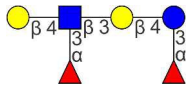
1218.44	1218.44	Hex4HexNAc2Fuc	β-D-Gal-(1→3/4)-β-D-GlcNAc (1→3/6)-β-D-Gal-(1→3/4)-[L-Fuc-(1→3/4)]-β-D-GlcNAc-(1→3/6)-β-D-Gal-(1→4)-β-D-Glc[a]	

a. Possible structures based on CID results and identified HMOs reported in references 13 and 14.

Analyst Accepted Manuscript

View Article Online
DOI: 10.1039/C7AN01397C

Published on 27 November 2017. Downloaded by University of Nottingham on 27/11/2017 21:14:28.

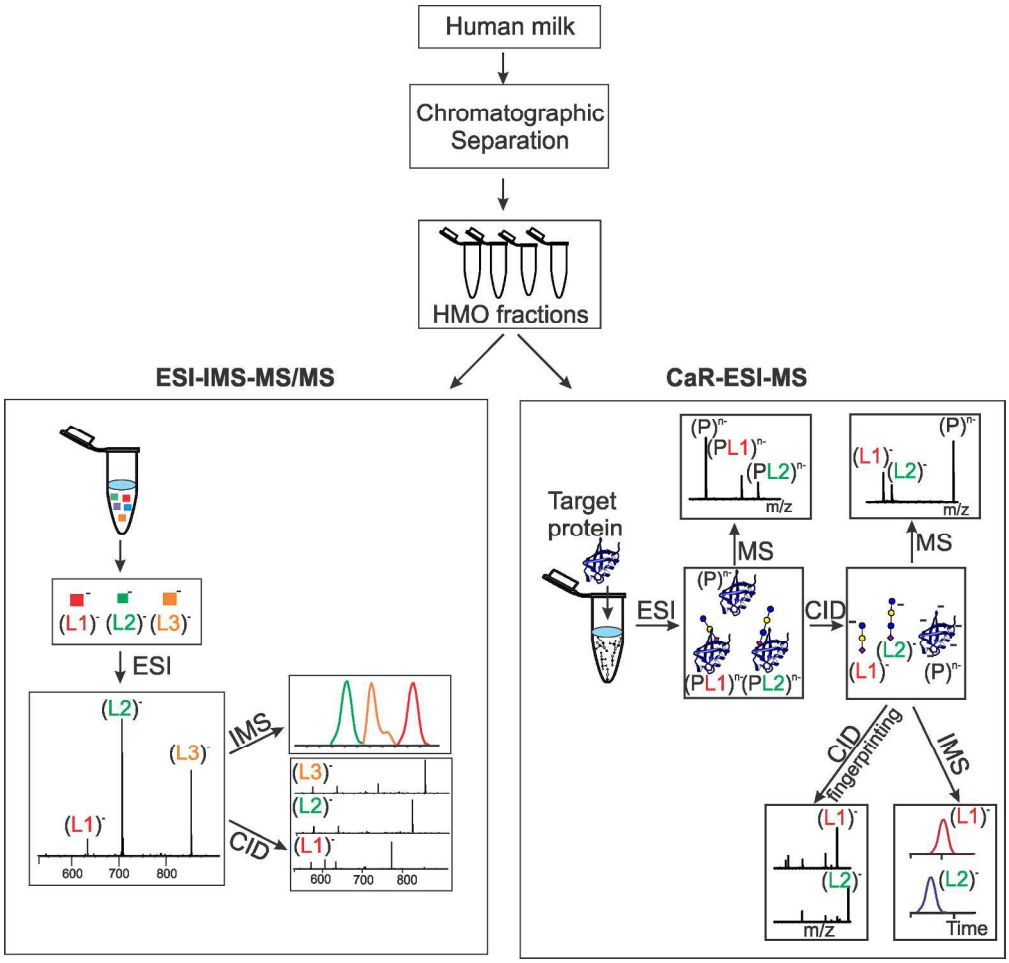

Figure 1. Overview of the two-step approach (ESI-IMS-MS/MS and CaR-ESI-MS) for screening HMO mixtures, extracted from human milk, against lectins.

Analyst Accepted Manuscript

View Article Online
DOI: 10.1039/C7AN01397C

Published on 27 November 2017. Downloaded by University of Nottingham on 27/11/2017 21:14:28.

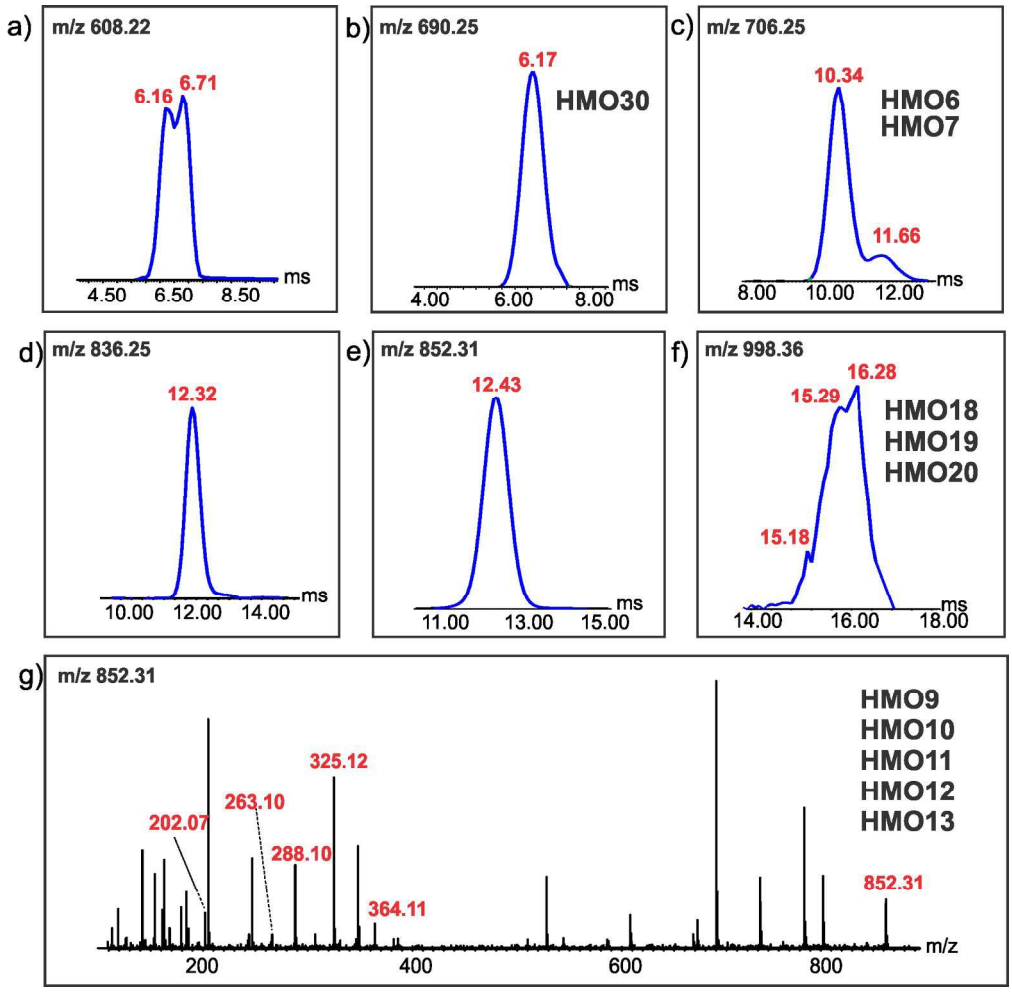

Figure 2. IMS-ATDs measured for the deprotonated HMO ions at (a) m/z 608.22; (b) m/z 690.25; (c) m/z 706.25; (d) m/z 836.25; (e) m/z 852.31 and (f) m/z 998.36 produced by ESI performed on an aqueous ammonium acetate solution (40 mM, pH 6.8) of *Fr2* (0.05 µg µL-1). (g) CID mass spectrum acquired in the Transfer region at 30 V for deprotonated HMO ions at m/z 852.31.

Analyst Accepted Manuscript

View Article Online
DOI: 10.1039/C7AN01397C

Published on 27 November 2017. Downloaded by University of Nottingham on 27/11/2017 21:14:28.

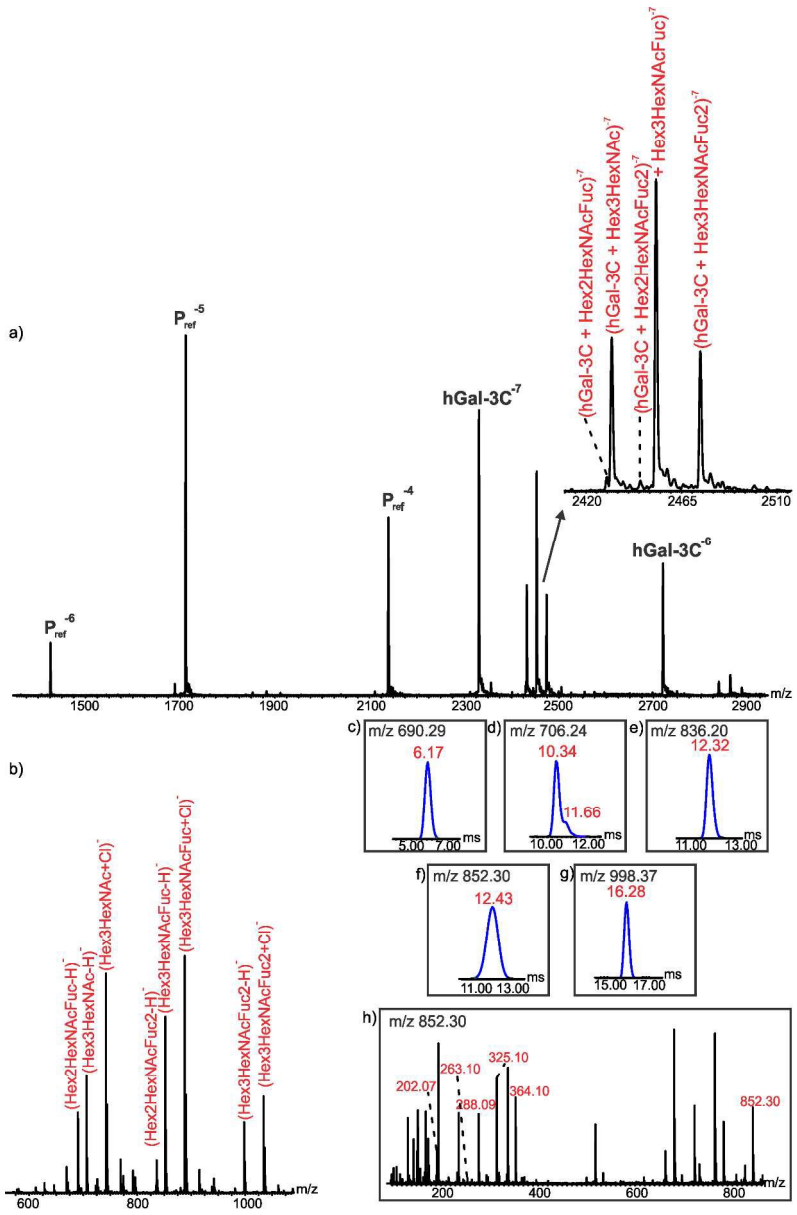

Figure 3. (a) Representative ESI mass spectra acquired in negative ion mode for 40 mM aqueous ammonium acetate solutions (pH 6.8) of P_{ref} (5 μM), *Fr2* (0.05 μg μL^{-1}) and hGal-3C (15 μM), (b) CID mass spectrum acquired for all (hGal-3C + HMO)$^{7-}$ ions at a Trap voltage of 40 V showing the released HMOs ligands; IMS-ATDs of (c) m/z 690.29 (d) m/z 706.24; (e) m/z 836.20; (f) m/z 852.30; (g) m/z 998.37; (h) CID mass spectrum acquired for released HMO anions with IMS-AT of 12.43 ms using a Transfer voltage of 30 V.

Analyst Accepted Manuscript

View Article Online
DOI: 10.1039/C7AN01397C

Published on 27 November 2017. Downloaded by University of Nottingham on 27/11/2017 21:14:28.

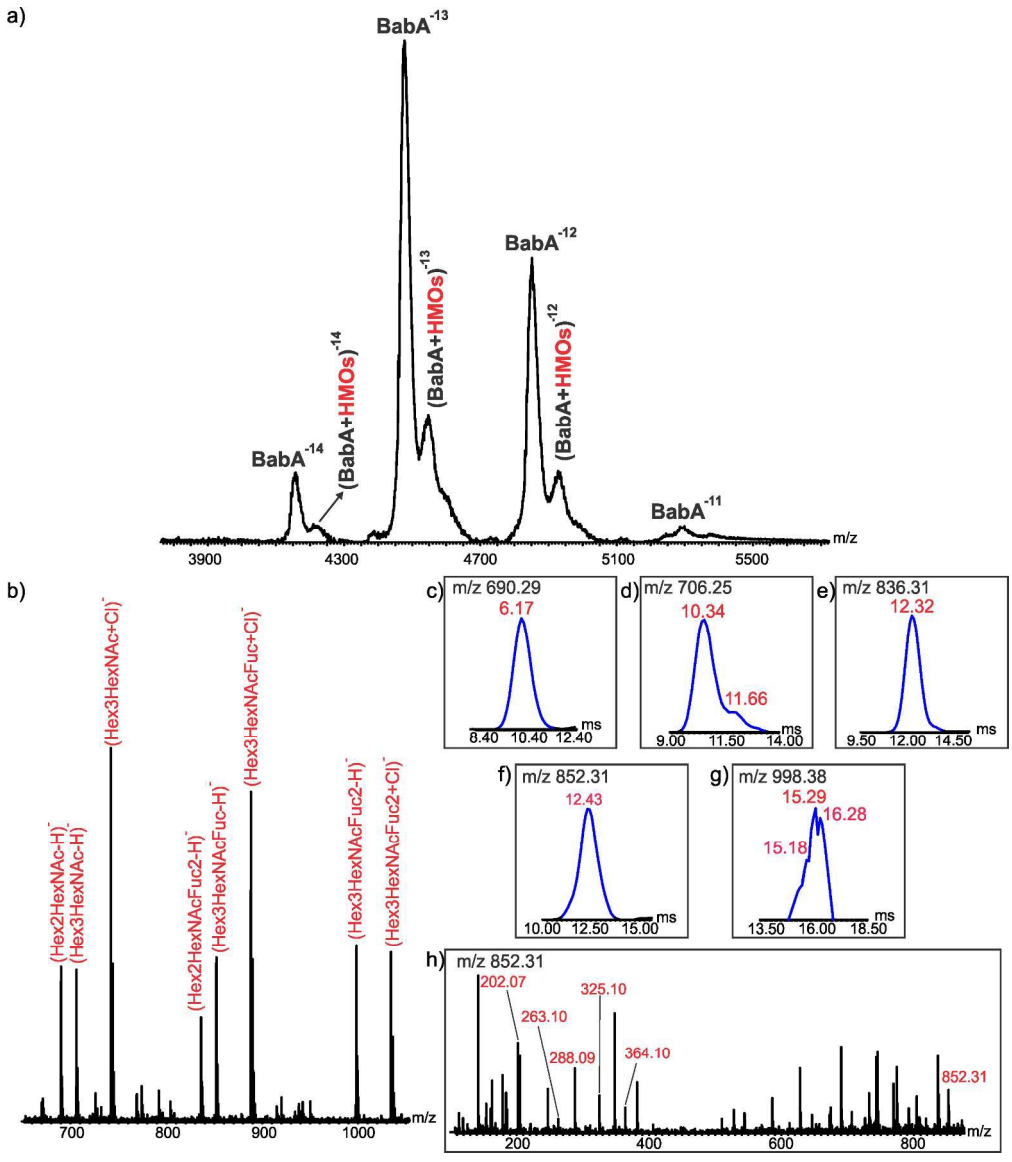

Figure 4. (a) Representative ESI mass spectra acquired in negative ion mode for 40 mM aqueous ammonium acetate solutions (pH 6.8) of *Fr2* (0.05 μg μL^{-1}) and BabA (5 μM), (b) CID mass spectrum acquired for all (BabA + HMO)$^{13-}$ ions at a Trap voltage of 90 V showing the released HMOs ligands; IMS-ATDs of (c) m/z 690.29 (d) m/z 706.25; (e) m/z 836.31; (f) m/z 852.31; (g) m/z 998.38; (h) CID mass spectrum acquired for released HMO anions with IMS-AT of 12.43 ms using a Transfer voltage of 30 V.

Analyst Accepted Manuscript

View Article Online
DOI: 10.1039/C7AN01397C

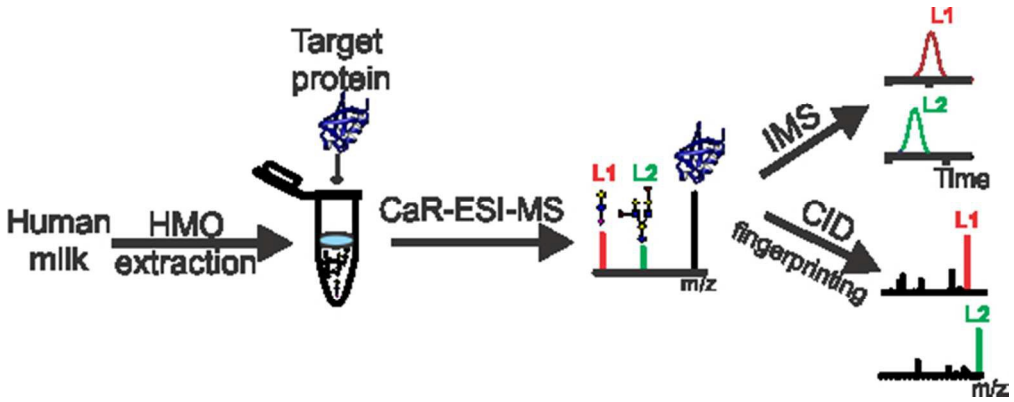

Published on 27 November 2017. Downloaded by University of Nottingham on 27/11/2017 21:14:28.

Analyst Accepted Manuscript